Inorganic Chemistry

pubs.acs.org/IC Article

Synthesis of Hydrated Ternary Lanthanide-Containing Chlorides Exhibiting X-ray Scintillation and Luminescence

Gyanendra B. Ayer, Mark D. Smith, Luiz G. Jacobsohn, Gregory Morrison, Hunter B. Tisdale, Logan S. Breton, Weiguo Zhang, P. Shiv Halasyamani, and Hans-Conrad zur Loye*



Cite This: Inorg. Chem. 2021, 60, 15371-15382



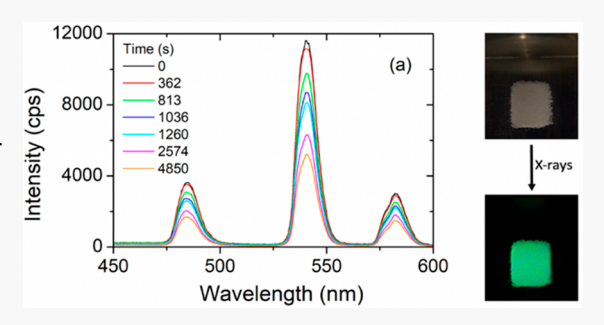
ACCESS

Metrics & More

Article Recommendations

Supporting Information

ABSTRACT: A series of new ternary lanthanide-based chlorides, $Cs_2EuCl_5(H_2O)_{10}$, $Cs_7LnCl_{10}(H_2O)_8$ (Ln = Gd or Ho), $Cs_{10}Tb_2Cl_{17}(H_2O)_{14}(H_3O)$, $Cs_2DyCl_5(H_2O)_6$, $Cs_8Er_3Cl_{17}(H_2O)_{25}$, and $Cs_5Ln_2Cl_{11}(H_2O)_{17}$ (Ln = Y, Lu, or Yb), were prepared as single crystals via a facile solution route. The compounds with compositions of $Cs_7LnCl_{10}(H_2O)_8$ (Ln = Gd or Ho) and $Cs_5Ln_2Cl_{11}(H_2O)_{17}$ (Ln = Y, Lu, or Yb) crystallize in a monoclinic crystal system in space groups C2 and $P2_1/c$, respectively, whereas $Cs_2EuCl_5(H_2O)_{10}$, $Cs_{10}Tb_2Cl_{17}(H_2O)_{14}(H_3O)$, and $Cs_8Er_3Cl_{17}(H_2O)_{25}$ crystallize in orthorhombic space groups Pbcm, Pnma, and $P2_12_1$, respectively. $Cs_2DyCl_5(H_2O)_6$ crystallizes with triclinic symmetry in space group $P\overline{1}$.



All of these compounds exhibit complex three-dimensional structures built of isolated lanthanide polyhedral units that are linked together by extensive hydrogen bonds. $Cs_2EuCl_5(H_2O)_{10}$ and $Cs_{10}Tb_2Cl_{17}(H_2O)_{14}(H_3O)$ luminesce upon irradiation with 375 nm ultraviolet light, emitting intense orange-red and green color, respectively, and $Cs_{10}Tb_2Cl_{17}(H_2O)_{14}(H_3O)$ scintillates when exposed to X-rays. Radioluminescence (RL) measurement of $Cs_{10}Tb_2Cl_{17}(H_2O)_{14}(H_3O)$ in powder form shows that the RL emission integrated in the range of 300–750 nm was ~16% of BGO powder.

■ INTRODUCTION

Scintillators, which are best known for the detection of ionizing radiation like X-rays and γ -rays, absorb and convert the highenergy ionizing radiation into visible light and have emerged as important materials in many different fields, including highenergy physics, medical imaging, positron emission tomography (PET),³ computer tomography (CT) scanners, radiation detection, and other industrial applications. Inorganic scintillators encompass a broad range of doped inorganic solids, such as NaI:Tl, CsI:Tl, LaBr₃:Ce³⁺, SrI₅:Eu²⁺, Cs₄CaI₆:Eu²⁺, and Cs₄SrI₆:Eu²⁺, as well as the self-activated materials, such as CaWO₄ and Bi₄Ge₃O₁₂ (BGO), which possess luminescent centers that are intrinsic to the structure.^{7–13} Recently, self-activated materials possessing a mixed oxide-halide environment have attracted attention, as the oxyfluoride environment around the metal centers tends to introduce distortions that can enhance their luminescence and scintillation behavior. 14,15 Hence, the investigation of novel oxide-halide materials as potential scintillators represents a promising area for the discovery of new oxyhalide materials for radiation detection.

Many halide-containing materials have been shown to exhibit excellent optical properties with high quantum yield due to their unique structural modularity ranging from zero- to three-dimensional (3D) networks. The inorganic copper(I)-based halides $Cs_3Cu_2X_5$ (X = Cl, Br, or I) exhibit intense

luminescent emission with a photoluminescence quantum yield of >90%, which is attributed to the highly efficient selftrapped excitonic effect caused by their structural distortion. 16 Furthermore, the metal halide-based perovskites are excellent X-ray scintillators and luminescent materials and have great potential for applications in the fields of optoelectronics and photodetectors, where their tunable band gaps, low-cost synthesis, wide color gamut, and structural flexibility make them highly attractive candidates. 17-20 The organic/inorganic hybrid halides, such as (PEA)₂PbBr₄, (C₃₈H₃₄P₂)MnBr₄, $[KC_2]_2[Cu_4I_6]$ (C = 12-crown-4 ether), and $(PPN)_2SbCl_5$ [PPN = bis(triphenylphosphoranylidene)ammonium cation], make up another promising class of scintillating materials, favored for their excellent photophysical properties that include a strong X-ray absorption coefficient and a facile solution synthesis. 21-24 Doping a lanthanide ion (Ln³⁺) into an inorganic halide compound is another facile approach for tuning their electronic properties across the visible light spectral region. The trivalent lanthanide ions as dopants exhibit

Received: July 2, 2021 Published: October 7, 2021





Table 1. Crystallographic Data for $Cs_2EuCl_5(H_2O)_{10}$, $Cs_7LnCl_{10}(H_2O)_8$ (Ln = Gd or Ho), $Cs_{10}Tb_2Cl_{17}(H_2O)_{14}(H_3O)$, $Cs_2DyCl_5(H_2O)_6$, $Cs_8Er_3Cl_{17}(H_2O)_{25}$, and $Cs_5Ln_2Cl_{11}(H_2O)_{17}$ (Ln = Y, Lu, or Yb)

	$\mathrm{Cs}_2\mathrm{EuCl}_5(\mathrm{H}_2\mathrm{O})_{10}$	$\mathrm{Cs}_7\mathrm{GdCl}_{10}(\mathrm{H}_2\mathrm{O})_8$	$\mathrm{Cs_7HoCl_{10}(H_2O)_8}$	$Cs_{10}Tb_2Cl_{17}(H_2O)_{14}(H_3O)$	$\mathrm{Cs_2DyCl_5}(\mathrm{H_2O})_6$	${\rm Cs_8Er_3Cl_{17}(H_2O)_{25}}$	$\mathrm{Cs}_{5}\mathrm{Y}_{2}\mathrm{Cl}_{11}(\mathrm{H}_{2}\mathrm{O})_{17}$	$\mathrm{Cs}_{5}\mathrm{Lu}_{2}\mathrm{Cl}_{11}(\mathrm{H}_{2}\mathrm{O})_{17}$	$Cs_5 Yb_2 Cl_{11} (H_2 O)_{17} \\$
formula weight	775.19	1586.25	1593.93	2520.84	713.67	2614.50	1538.59	1710.71	1701.81
crystal system	orthorhombic	monoclinic	monoclinic	orthorhombic	triclinic	orthorhombic	monoclinic	monoclinic	monoclinic
space group, Z	Рьст	C2	C2	Pnma	$p\overline{1}$	$P2_12_12_1$	$P2_1/c$	$P2_1/c$	$P2_1/c$
g(A)	7.7917(2)	18.1863(7)	18.1393(5)	18.1569(5)	8.3141(3)	9.5329(4)	23,1390(8)	23.0503(10)	23.0932(7)
b (Å)	13.7075(4)	9.3476(3)	9.3216(3)	17.8077(5)	9.3997(3)	23.1485(9)	19.0032(6)	18.9377(8)	18.9550(6)
c (Å)	18.3357(5)	9.4878(3)	9.4612(3)	16.5082(5)	9.9928(3)	27.5822(11)	18.2747(7)	18.1628(7)	18.2008(5)
$\alpha \; (\deg)$	06	06	06	06	87.4220(10)	06	06	06	06
β (deg)	06	94.0870(10)	94.0330(10)	06	88.5510(10)	06	93.6790(10)	93.5600(15)	93.5676(12)
γ (deg)	06	06	06	06	89.9770(10)	06	06	06	06
$V\left(\mathring{\mathbf{A}}^{3}\right)$	1958.34(9)	1608.81(10)	1595.81(8)	5337.6(3)	779.90(4)	6086.6(4)	8019.1(5)	7913.1(6)	7951.6(4)
$ ho_{ m calcd}~({ m g/cm^3})$	2.629	3.275	3.317	3.137	3.039	2.853	2.549	2.872	2.843
$\mu (\mathrm{mm}^{-1})$	7.575	10.717	11.206	10.239	10.246	9.615	8.134	10.285	9.973
radiation $[\lambda \ (ext{Å})]$	Mo K α (0.71073)								
T(K)	100(2)								
crystal dimensions	$0.180 \text{ mm} \times 0.160$ mm $\times 0.080 \text{ mm}$	$0.220 \text{ mm} \times 0.120 \text{ mm} \times 0.080 \text{ mm}$	$0.280 \text{ mm} \times 0.240$ mm $\times 0.180 \text{ mm}$	0.160 mm × 0.130 mm × 0.060 mm	$0.100 \text{ mm} \times 0.060$ mm $\times 0.040 \text{ mm}$	$0.340 \text{ mm} \times 0.300 \text{ mm} \times 0.200 \text{ mm}$	$0.200 \text{ mm} \times 0.160 \text{ mm} \times 0.060 \text{ mm}$	$0.320 \text{ mm} \times 0.240 \text{ mm} \times 0.200 \text{ mm}$	$0.080 \text{ mm} \times 0.060 \text{ mm} \times 0.060 \text{ mm}$
2θ range (deg)	2.614-37.825	2.152-40.293	2.158-40.247	2.022-35.052	2.169-37.860	2.260-35.019	1.816-33.182	2.963-40.094	2.324-37.765
Flack parameter	I	0.025 (2)	0.046 (4)	I	I	0.017 (2)	I	I	I
no. of reflections collected	96240	137281	59353	197049	109155	366894	333217	716320	822715
data/ restraints/ parameters	5399/0/130	10177/9/150	10033/17/149	12104/22/284	8409/12/176	22181/81/655	30636/47/882	49815/49/878	42696/48/874
$R_{ m int}$	0.0388	0.0359	0.0554	0.0740	0.0352	0.0811	0.0632	0.1126	0.0712
goodness of fit	1.134	1.259	1.168	1.043	1.262	1.166	1.044	1.036	1.047
R_1 $[I > 2\sigma(I)]$	0.0148	0.0112	0.0207	0.0232	0.0118	0.0304	0.0421	0.0307	0.0247
wR_2 (all data)	0.0280	0.0248	0.0486	0.0440	0.0248	0.0741	0.0456	0.0548	0.0498

characteristic sharp emission peaks that can be tuned due to their flexible coordination geometries and their size-imposed preference for high-coordination number environments ($CN \ge$ 6). To date, numerous lanthanide-doped halide nanocrystals and quantum dots have been prepared and reported to impart intense luminescent properties across the visible range, and as a result, many have found their way into applications, including television sets, bioimaging, and fluorescent lights.^{25–27} Moreover, lanthanide-doped metal chlorides, such as Tl₂GdCl₅:Ce³⁺, have been reported as X-ray and γ-ray scintillators with a light yield of ~53000 photons/MeV.²⁸ Interestingly, while halide materials containing lanthanides as an intrinsic luminescent center have been reported to display excellent optical properties, they have not been investigated as extensively, and only very few compounds of this type have been studied to date.29

Herein, we report on a series of three- and two-dimensional structured ternary lanthanide-containing chlorides belonging to six different structure types, namely, Cs₂EuCl₅(H₂O)₁₀, $C s_7 L n C l_{10} (H_2 O)_8 (L n = G d or H o),$ $Cs_{10}Tb_{2}Cl_{17}(H_{2}O)_{14}(H_{3}O), Cs_{2}DyCl_{5}(H_{2}O)_{6},$ $Cs_8Er_3Cl_{17}(H_2O)_{25}$, and $Cs_5Ln_2Cl_{11}(H_2O)_{17}$ (Ln = Y, Lu, or Yb), that can be easily synthesized via solution routes at room temperature. Within this series, we observed that single crystals of $Cs_2EuCl_5(H_2O)_{10}$ and $Cs_{10}Tb_2Cl_{17}(H_2O)_{14}(H_3O)$ exhibit sharp optical emissions under long-wavelength ultraviolet (UV) light with orange-red and green colors that are typical of Eu34 and Tb3+ ions, respectively. Moreover, the Cs₁₀Tb₂Cl₁₇(H₂O)₁₄(H₃O) compound scintillates emitting intense green light when irradiated by laboratory X-rays, validating the premise that new scintillators can be discovered among the extended lanthanide halide family.

■ EXPERIMENTAL SECTION

Reagents. CsCl (Alfa Aesar, 99%), LnCl₃·6H₂O (Ln = Y, Lu, Eu, Gd, Tb, Dy, Ho, Er, or Yb) (Alfa Aesar, 99.9%), and HCl (Sigma-Aldrich, 37%), were used as received.

Synthesis. Single crystals of the titled compounds were synthesized by evaporating a dilute hydrochloric acid solution (4 M) containing a mixture of $LnCl_3 \cdot 6H_2O$ (Ln = Y, Lu, Eu, Gd, Tb, Dy, Ho, Er, or Yb) and CsCl at room temperature. For the preparation of these compounds, 4 mmol of CsCl and 1 mmol of LnCl₃·6H₂O (Ln = Y, Lu, Eu, Gd, Tb, Dy, Ho, Er, or Yb) were combined with 1 mL of H₂O and 0.5 mL of 12 M HCl. The respective solutions were placed in a 23 mL PTFE liner, stirred slowly to completely dissolve the reagents, and then left in the fume hood for 48 h to slowly evaporate the water at room temperature. Evaporation of the solution resulted in the formation of large block single crystals of the respective compounds. All compounds were found to be sensitive to air and moisture when removed from their mother liquor with single crystals decomposing over the course of several hours. Furthermore, the reaction was found to be dependent on the ambient humidity. The reported reactions were performed in the winter months when the humidity in the laboratory was low. Reproduction of Cs₁₀Tb₂Cl₁₇(H₂O)₁₄(H₃O) synthesis during the humid summer months required either gentle heating of the PTFE liner or placing the liner in a sealed container surrounded by desiccant. The mother liquor was very hygroscopic, quickly picked up atmospheric water, and redissolved the crystals when removed from the hot plate or desiccant.

Single-Crystal X-ray Diffraction. X-ray intensity data from single crystals were collected at 100(2) K under liquid N₂ using a Bruker D8 QUEST diffractometer equipped with a PHOTON-II area detector and an Incoatec microfocus source (Mo Kα radiation; λ = 0.71073 Å). The raw area detector data frames were reduced, scaled, and corrected for absorption effects using the Bruker programs APEX3, SAINT+, and SADABS.^{30,31} The structure was determined

with SHELXT.³² Subsequent difference Fourier calculations and full-matrix least-squares refinement against F^2 were performed with SHELXL-2018³³ using OLEX2.³⁴ The crystallographic data and the results of the diffraction experiments are summarized in Table 1.

Powder X-ray Diffraction. Powder X-ray diffraction (PXRD) data for $Cs_{10}Tb_2Cl_{17}(H_2O)_{14}(H_3O)$ (Figure S1) were collected on a Rigaku SmartLab Diffractometer in transmission geometry using a Mo $K\alpha$ rotating anode (45 kV, 200 mA; λ = 0.70932 Å). Single crystals of $Cs_{10}Tb_2Cl_{17}(H_2O)_{14}(H_3O)$ were ground under their mother liquor, quickly loaded in a polyimide tube with an inner diameter of 0.31 mm and an outer diameter of 0.36 mm, and sealed with nitrocellulose cement. This tube was then placed in a borosilicate glass capillary with an outer diameter of 1.0 mm. Data were collected from 2θ = 5° to 25° with 0.01° steps. The diffraction pattern was analyzed, fitted, and refined with the Rietveld/d-I pattern method using the Rigaku SmartLab Studio II software.

Energy-Dispersive Spectroscopy (EDS). EDS was performed on product single crystals using a Tescan Vega-3 scanning electron microscope (SEM) equipped with a Thermo EDS attachment. The SEM was operated in low-vacuum mode. Crystals were mounted on an SEM stud with carbon tape and analyzed using a 20 kV accelerating voltage and a 30 s accumulating time. The SEM images and EDS data are shown in Figure S2 and Table S1, respectively.

Optical Properties. Microphotoluminescence data were collected on a Horiba Micro-SPEX system equipped with a Horiba iHR320 imaging spectrograph and a Syncerity CCD detector. Excitation was provided by a confocal 375 nm diode laser. Data were collected using Labspec 6 in the range of 400–800 nm with a laser excitation source power of 0.4 mW and a 10× UV objective.

Scintillation. Radioluminescence (RL) measurements were taken using a customer-designed configuration of the Freiberg Instruments Lexsyg Research spectrofluorometer equipped with a Varian Medical Systems VF-50J X-ray tube with a tungsten target. The X-ray source was coupled with an ionization chamber for continuous radiation intensity monitoring. The light emitted by the sample was collected by an Andor Technology SR-OPT-8024 optical fiber connected to an Andor Technology Shamrock 163 spectrograph coupled to a cooled (-80 °C) Andor Technology DU920P-BU Newton CCD camera (spectral resolution of ~0.5 nm/pixel). Powders filled ~8 mm diameter, 0.5 mm deep cups, thus allowing for relative RL intensity comparison between different samples. Bismuth germanium oxide (BGO) powder [Alfa Aesar Puratronic, 99.9995% (metal basis)] was used as a reference. RL was measured under continuous X-ray irradiation (40 kV, 1 mA) with an integration time of 1 or 5 s. Spectra were corrected by the built-in wavelength response of the system. To ensure phase stability during sample shipment, the prepared sample was shipped on dry ice.

■ RESULTS AND DISCUSSION

Crystal Growth. The use of HCl in the reaction mixture aided in the dissolution of reagents, analogous to the role of HF in the mild hydrothermal synthesis of fluorides.^{35–38} Single crystals of hydrated ternary alkali lanthanide chloride compounds were grown via precipitation from an aqueous solution by slow evaporation of the liquid at room temperature, an approach that had already been found to be extremely effective for crystallizing numerous hydrated ternary fluorides and chlorides exhibiting various structural motifs. 39-41 Despite using almost identical reaction conditions for all compositions studied, starting with the lanthanide chloride precursors, the reaction products were found to be quite varied, crystallizing with different compositions and in different structure types. The most likely cause of this variation among the chemically rather similar lanthanides is likely to be found in the lanthanide contraction. It is well established that the later lanthanides, due to their smaller sizes, tend to adopt coordination numbers lower than those of the early lanthanides. As an illustration,

Klepov et al. have reported that in the extended lanthanide series of $NaLnP_2S_6$ (Ln = La, Ce, or Pr) and $CsLnP_2F_7$ (Ln = Nd-Yb or Y), the early lanthanides take on 9-fold coordination, while the later lanthanide cations favor a coordination number of 8^{42} . These high coordination numbers, combined with the tendency of lanthanides to be quite flexible when it comes to the geometry of their coordination environment, can readily cause uniform reaction conditions to result in different compositions and crystal structures. In this study, hydrated ternary alkali lanthanide chlorides were crystallized for Eu-Lu as well as for Y. All attempts to obtain similar ternary chloride materials containing the early lanthanides (La-Sm) using the same reaction condition were unsuccessful in yielding new compositions and, instead, resulted in only crystalline products already reported in the literature.

Crystal Structures. The lanthanide chloride series crystallize in six different structure types, Cs₂EuCl₅(H₂O)₁₀, C s $_{7}$ L n C l $_{10}$ (H $_{2}$ O) $_{8}$ (L n = G d or H o), C s $_{10}$ T b $_{2}$ C l $_{17}$ (H $_{2}$ O) $_{14}$ (H $_{3}$ O), C s $_{2}$ D y C l $_{5}$ (H $_{2}$ O) $_{6}$, C s $_{8}$ Er $_{3}$ C l $_{17}$ (H $_{2}$ O) $_{25}$, and C s $_{5}$ L n $_{2}$ C l $_{11}$ (H $_{2}$ O) $_{17}$ (Ln = Y, Lu, or Yb). In this study, we observed that on moving across the lanthanide series (Eu-Lu), the symmetry of the compounds changes and the coordination number of the lanthanide cations decreases from 9 to 8, as a consequence of lanthanide contraction, resulting in six different compositions. By comparison, this effect was observed by Klepov et al. where a minor change in size between the lanthanide cations causes a sharp change in the coordination environment and coordination number, resulting in different structure types. 43 The lanthanide chloride compounds, although having different symmetries and compositions, all consist of lanthanide polyhedra that are isolated from each other but linked into a complex structure by Cs-Cl/Cs-O bonds and by extensive OH-O hydrogen bonding and OH-Cl interactions.

 $Cs_2EuCl_5(H_2O)_{10}$. $Cs_2EuCl_5(H_2O)_{10}$ crystallizes in the monoclinic crystal system in space group Pbcm. The asymmetric unit consists of two cesium atoms, one europium atom, three chlorine atoms, and six water molecules. Eu is nine-coordinated, exclusively by water. The $Eu(H_2O)_9$ polyhedra are isolated from each other but linked to Cs atoms through bridging waters. Overall, it is a threedimensional framework, assisted by OH-O hydrogen bonds and OH-Cl interactions. The Eu site forms an Eu(H₂O)₉ coordination polyhedron (Figure 1a) in the shape of a tricapped trigonal prism with Eu-O bond lengths of 2.4701(9)-2.4775(10) Å and O-Eu-O angles of 66.36(3)-144.20(4)°. The Cs cations are coordinated by both chlorine atoms and water molecules, and the bond lengths for Cs-Cl and Cs-O range from 3.4554(3) to 3.7070(5) Å and from 3.1567(17) to 3.7686(18) Å, respectively. The Cs cations are located within the voids and connect the isolated polyhedral units by corner sharing through O atoms of the water molecules to form a 3D framework structure (Figure 1b).

 $Cs_{10}Tb_2Cl_{17}(H_2O)_{14}(H_3O)$. The compound crystallizes in the orthorhombic system. The pattern of systematic absences in the intensity data was consistent with space group Pnma, which was confirmed by structure solution. The asymmetric unit consists of one terbium atom, eight cesium atoms, 10 chloride atoms, and nine oxygen atoms. Tb is eight-coordinated by six H_2O molecules and two Cl atoms. The $Tb(H_2O)_6Cl_2$ polyhedra are isolated from each other but linked into a complex 3D structure via all of the Cs and Cl ions and a

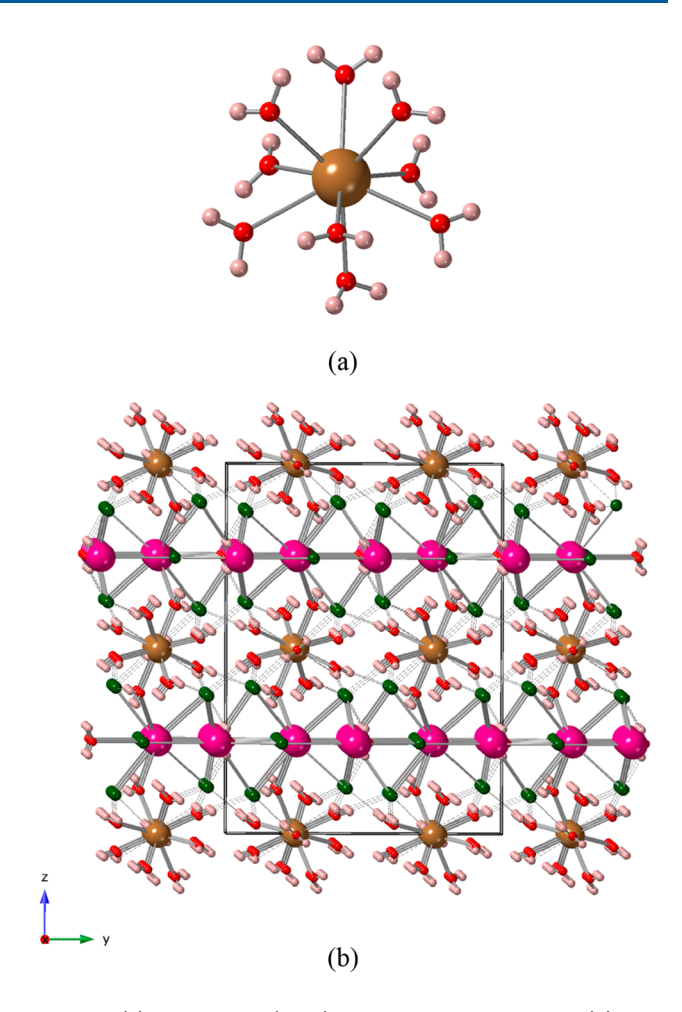


Figure 1. (a) View of a $\operatorname{Eu}(H_2O)_9$ coordination polyhedron. (b) View of the 3D structure of $\operatorname{Cs}_2\operatorname{EuCl}_5(H_2O)_{10}$ along the a axis. The cesium, europium, oxygen, chlorine, and hydrogen atoms are colored pink, brown, red, dark green, and off-white, respectively. The black box outlines the unit cell.

network consisting of OH-O hydrogen bonds and OH-Cl interactions. In the crystal structure, the Tb atoms form Tb(H₂O)₆Cl₂ coordination polyhedra with Tb-Cl bond lengths of 2.7041(9)-2.7091(8) Å and Tb-O bond lengths of 2.373(2)-2.4525(17) Å. The bond angles of the Tb polyhedra fall within the wide range of $67.78(7)-149.80(5)^{\circ}$ forming a distorted square antiprism (Figure 2a). The Cs1-Cs2, Cl1-Cl7, and O1-O6 are located at positions of general crystallographic symmetry (Wyckoff site 8d), whereas Cs3-Cs8, Cl8-Cl10, and O7-O9 are located on or are disordered across (O9) mirror planes (Figure S3). The presence of a hydronium ion is consistent with the composition determined from the heavy atoms, which requires an additional +1 charge for charge balance. The three hydronium H atoms also form a typical network of OH-O hydrogen bonds and OH-Cl interactions, providing further support for the H₃O⁺ assignment. The isolated metal polyhedra are connected to Cs cations located in the voids through corner-shared Cl atoms as well as by an extensive hydrogen bonding network to form a 3D framework structure (Figure 2b).

 $Cs_7LnCl_{10}(H_2O)_8$ ($Ln = G\bar{d}$ or Ho). The two compounds are isostructural and show only minor differences in their unit cell lattice parameters. The $Cs_7LnCl_{10}(H_2O)_8$ ($Ln = G\bar{d}$ or Ho) compounds crystallize in the monoclinic crystal system and

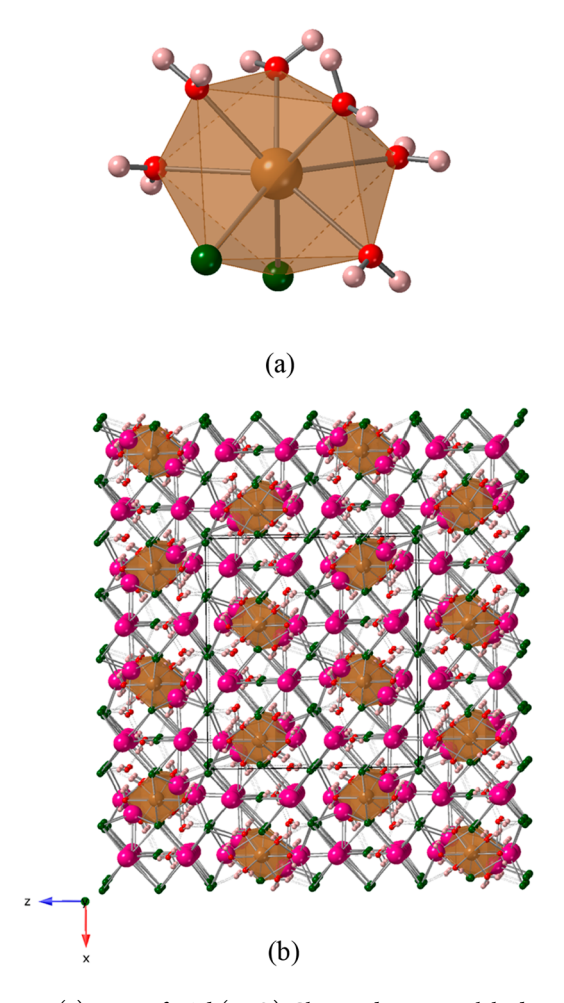


Figure 2. (a) View of a $Tb(H_2O)_6Cl_2$ coordination polyhedron. (b) View of the 3D structure of $Cs_{10}Tb_2Cl_{17}(H_2O)_{14}(H_3O)$ along the b axis. The cesium, terbium, oxygen, chlorine, and hydrogen atoms are colored pink, brown, red, dark green, and off-white, respectively. The black box outlines the unit cell.

adopt an acentric space group C2. SHG measurements were attempted to confirm the noncentrosymmetric nature of this structure, as well as the Cs₈Er₃Cl₁₇(H₂O)₂₅ structure (vide infra). However, the extreme water sensitivity of these compounds inhibited the reliable measurement of SHG activity. The asymmetric unit in C2 consists of one Ln atom, four cesium atoms, five chlorine atoms, and four water molecules. The unique Ln atom has an 8-fold Ln(H2O)6Cl2 coordination environment (Figure 3a). The 3D crystal structure is built of the isolated Ln polyhedra that are connected to each other by OH-O hydrogen bonds and OH-Cl interactions. The Ln site forms an eight-coordinate Ln(H₂O)₆Cl₂ polyhedron with Ln-Cl and Ln-O bond lengths ranging from 2.7228(8) to 2.7540(4) Å and from 2.339(3) to 2.4362(15) Å, respectively. The compound has a Cs/Cl rich composition, and the isolated metal polyhedra are linked by corner-sharing Cs-Cl bonds as well as extensive hydrogen bonding to form a 3D framework structure (Figure 3b).

 $Cs_2DyCl_5(H_2O)_6$. The compound crystallizes in the triclinic crystal system in centrosymmetric space group $P\overline{1}$. The asymmetric unit consists of one Dy atom, two cesium atoms, five chlorine atoms, and six water molecules. The unique Dy site is eight-coordinate $DyCl_2(H_2O)_6$ (Figure 4a). This is a

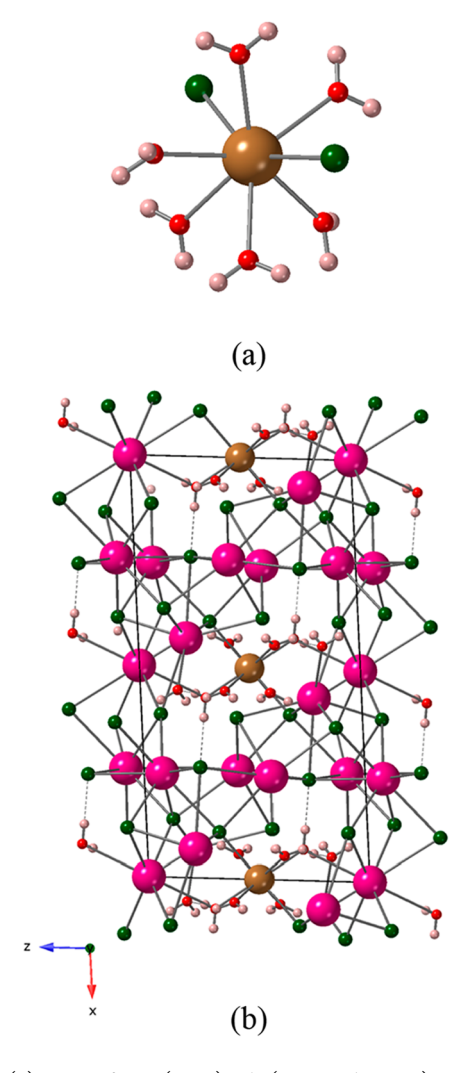


Figure 3. (a) View of a $\text{Ln}(\text{H}_2\text{O})_6\text{Cl}_2$ (Ln = Gd or Ho) coordination polyhedron. (b) View of the 3D structure of $\text{Cs}_7\text{Ln}\text{Cl}_{10}(\text{H}_2\text{O})_8$ (Ln = Gd or Ho) along the b axis. The cesium, Ln (Ln = Gd or Ho), oxygen, chlorine, and hydrogen atoms are colored pink, brown, red, dark green, and off-white, respectively. The black box outlines the unit cell.

two-dimensional (2D) layered structure where the layers orient parallel to the a-b plane and stack along [001] via extensive OH–Cl interactions. The nonhydrated form, Cs2DyCl₅, has been reported in the literature and exhibits orthorhombic symmetry. The Dy cation forms a DyCl₂(H₂O)₆ coordination polyhedron with Dy–Cl and Dy–O bond lengths ranging from 2.7016(3) to 2.7112(3) Å and from 2.3501(9) to 2.4382(8) Å, respectively. The Cs atoms take on a CsCl₇(H₂O) coordination sphere and are linked to neighboring cesium and dysprosium units through corner-shared chlorine and oxygen atoms to form a layer in the a-b plane (Figure 4b). These layers are further connected to each other by OH–Cl interactions to form a 2D layered structure (Figure 4c).

 $Cs_8Er_3Cl_{17}(H_2O)_{25}$. It is a fairly large structure with a unit cell volume of 6100 Å³ and noticeably different from the other structures. The compound crystallizes in the orthorhombic crystal system and adopts the acentric space group $P2_12_12_1$, which allows for chirality. The asymmetric unit consists of three crystallographically unique erbium atoms, eight cesium

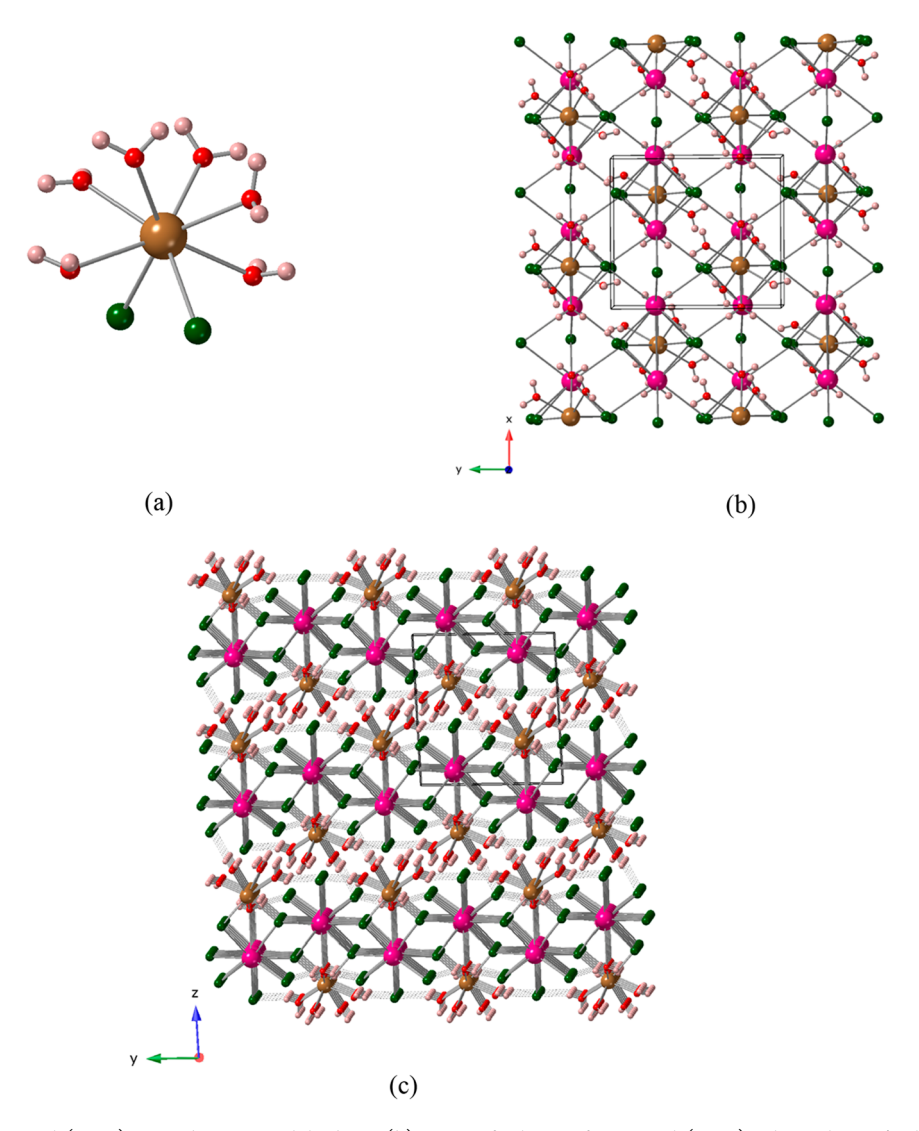


Figure 4. (a) View of a $DyCl_2(H_2O)_6$ coordination polyhedron. (b) View of a layer of $Cs_2DyCl_5(H_2O)_6$ along the a-b plane. (c) View of a 2D layered structure of $Cs_2DyCl_5(H_2O)_6$ consisting of the layers parallel to the a-b plane and stacking along [001] via extensive OH–Cl hydrogen bonding. The cesium, dysprosium, oxygen, chlorine, and hydrogen atoms are colored pink, brown, red, dark green, and off-white, respectively. The black box outlines the unit cell.

atoms, 17 chlorine atoms, and 25 water oxygen atoms. Of the three unique Er atoms, two have ErCl(H₂O)₇ coordination polyhedra and one has an Er(H₂O)₈ coordination polyhedron (Figure 5a) with Er-Cl and Er-O bond lengths ranging from 2.6513(17) to 2.6616(16) Å and from 2.299(5) to 2.409(5) Å, respectively. The Cs cations connect to each other through both corner- and edge-shared Cl atoms as well as cornershared O atoms to form the Cs/Cl/H2O framework that contain large channels in which the Er polyhedra reside (Figure 5b). These polyhedra are isolated from one another but engage in extensive OH-O hydrogen bonding and especially numerous OH-Cl interactions with the Cs/Cl/ H₂O framework to form a 3D crystal structure (Figure 5c). Some minor disorder exists, evident in a split chloride position and partial occupancy of a nearby water oxygen (Figure S4), where Cl9A and Cl9B hold an 80/20 split position and O25A is 80% occupied to prevent steric overlap with Cl9B.

 $Cs_5Ln_2Cl_{11}(H_2O)_{17}$ (Ln = Y, Lu, or Yb). The $Cs_5Ln_2Cl_{11}(H_2O)_{17}$ (Ln = Y, Lu, or Yb) compounds crystallize in the monoclinic system and represent the isostructural series.

The pattern of systematic absences in the intensity data was uniquely consistent with space group $P2_1/c$, which was verified by the structure solution. It is a complex structure consisting of 10 unique cesium atoms, four unique lanthanide atoms, 22 unique chlorine atoms, and a total of 34 unique water oxygen atoms. The four Ln cations are eight-coordinate. Two have $Ln(H_2O)_7Cl$ coordination spheres, and two have $Ln(H_2O)_8$ coordination spheres (Figure 6a) with Ln-Cl and Ln-O bond lengths ranging from 2.6576(5) to 2.6978(6) Å and from 2.252(2) to 2.3887(19) Å, respectively. These spheres are isolated from each other but linked together by Cs-Cl/Cs-O bonds and with extensive OH-O hydrogen bonds and OH-Cl interactions to form a 3D crystal structure (Figure 6b,c). There is extensive disorder surrounding the Ln4 site (Figure S5). A total of eight water oxygens coordinated to Ln4 were located. Three (O23-O25) are not disordered and refined normally. The remaining Ln4 coordination sites are occupied by nine half-occupied oxygen atoms (O26A, O27A/B, O28A/ B, O29A, and O30A-C) and two one-quarter-occupied (O29B/C) oxygen atoms. The disorder can be interpreted as

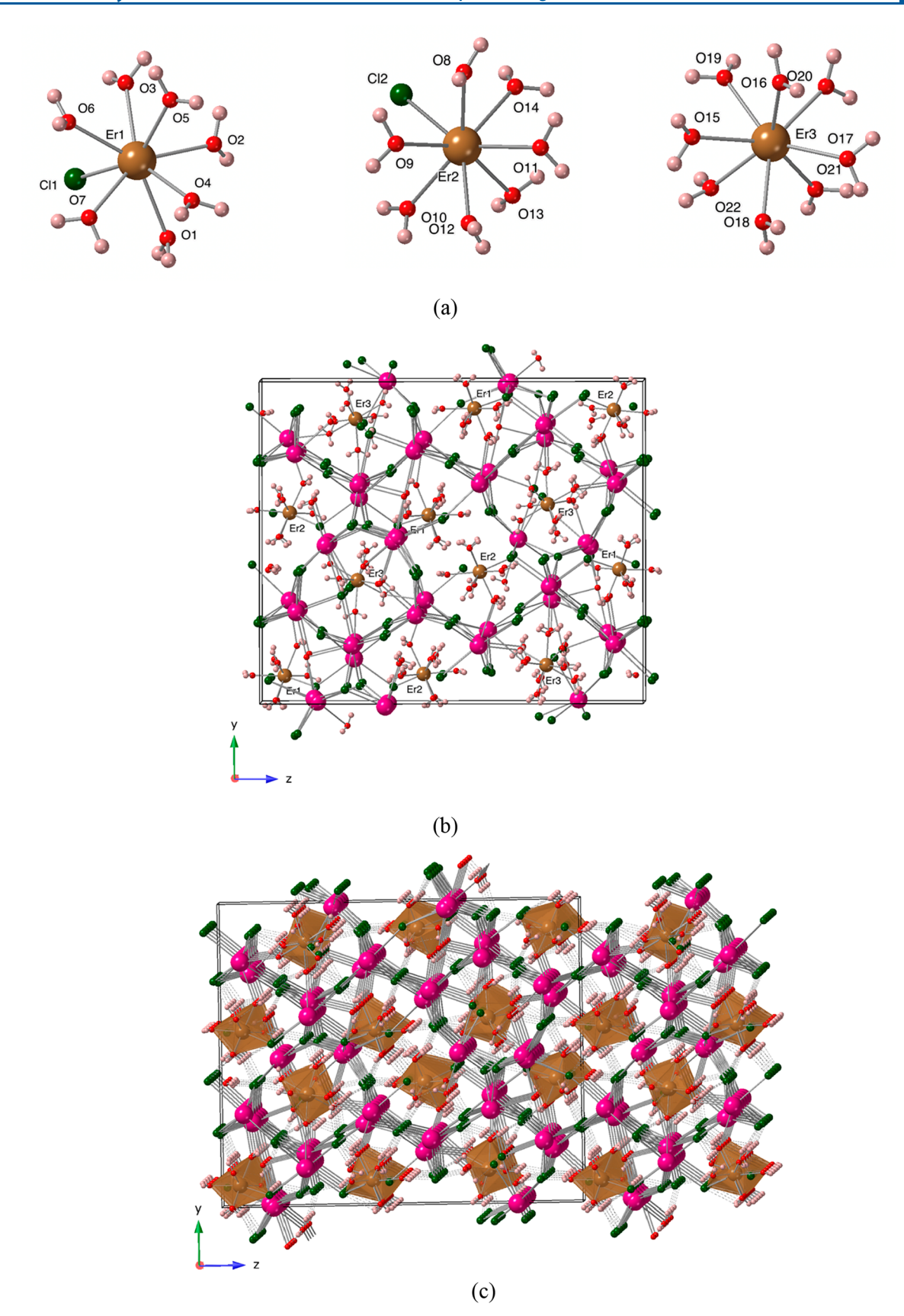


Figure 5. (a) View of $ErCl(H_2O)_7$ and $Er(H_2O)_8$ coordination polyhedra with three unique Er atoms. (b) View of a $Cs/Cl/H_2O$ framework along the a axis. (c) View of a 3D structure of $Cs_8Er_3Cl_{17}(H_2O)_{25}$ along the a axis. The cesium, erbium, oxygen, chlorine, and hydrogen atoms are colored pink, brown, red, dark green, and off-white, respectively. The black box outlines the unit cell.

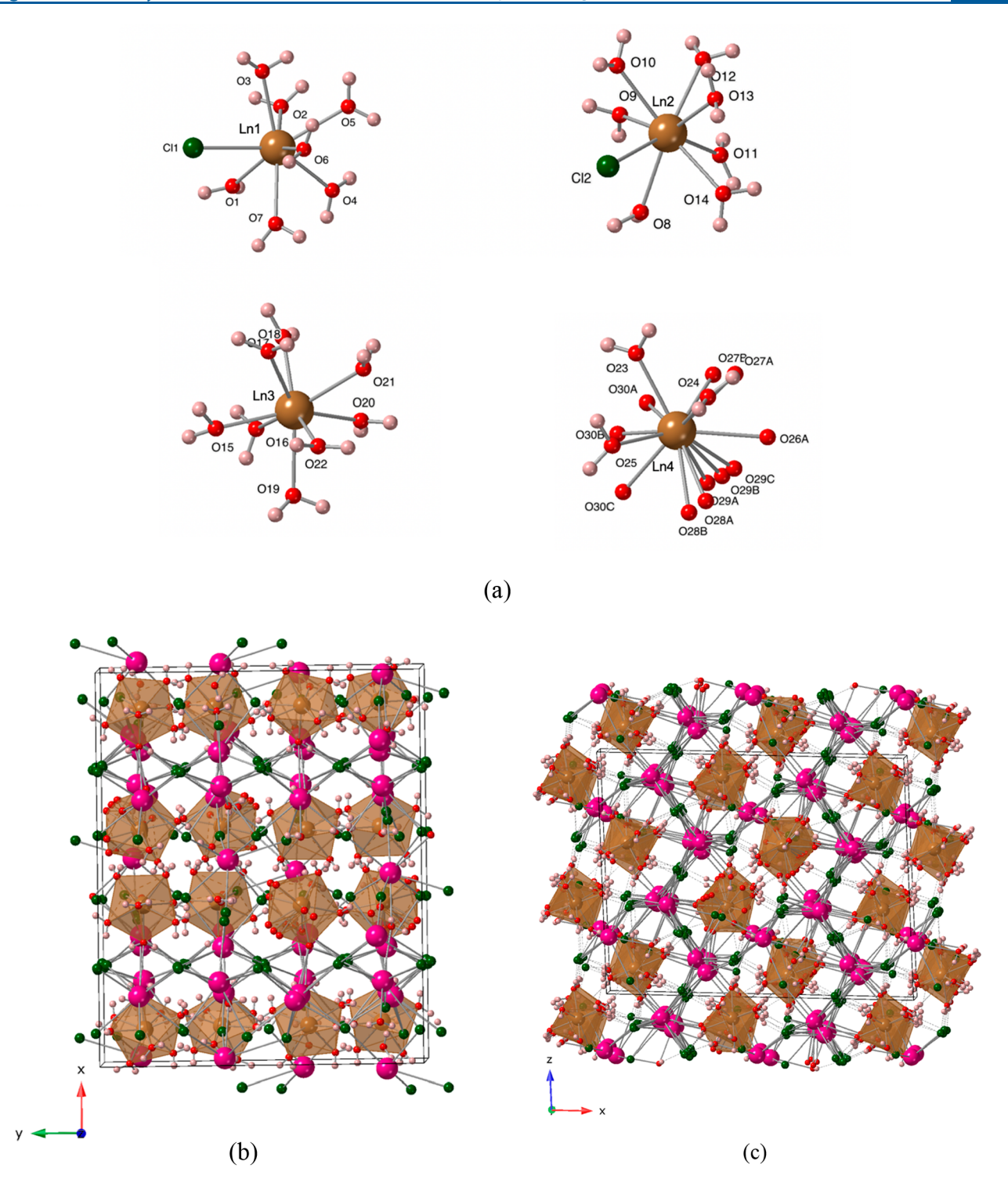


Figure 6. (a) View of $LnCl(H_2O)_7$ and $Ln(H_2O)_8$ coordination polyhedra with four unique Ln atoms. (b and c) View of a 3D structure of $Cs_5Ln_2Cl_{11}(H_2O)_{17}$ along the c and b axes, respectively. The cesium, Ln (Ln = Y, Lu, or Yb), oxygen, chlorine, and hydrogen atoms are colored pink, brown, red, dark green, and off-white, respectively. The black box outlines the unit cell.

two ${\rm Ln(H_2O)_8}^{3+}$ cations disordered over two orientations, each with 50% occupancy. O23–O25 are common to both disorder components. One orientation, involving O29B/C, is further split into equally two components, but only one coordination site is affected (O29B/C).

Optical Properties. The luminescence spectrum for $Cs_2EuCl_5(H_2O)_{10}$ is shown in Figure 7a. Under 365 nm UV light excitation, the emission spectrum consists of several

intense and weak emission peaks that are typical for the characteristic transitions of Eu³+-based compounds. 45,46 The most intense emission peak is centered at ${\sim}610$ nm that arises due to the $^5D_0-^7F_2$ transition. The emission spectrum consists of two other relatively intense peaks and several weak peaks corresponding to the $^5D_0-^7F_1$ (${\sim}588$ nm), $^5D_0-^7F_4$ (${\sim}695$ nm), $^5D_0-^7F_3$ (${\sim}650$ nm), $^5D_1-^7F_0$ (524 nm), $^5D_1-^7F_1$ (${\sim}536$ nm), and $^5D_1-^7F_2$ (555 and 558 nm) transitions,

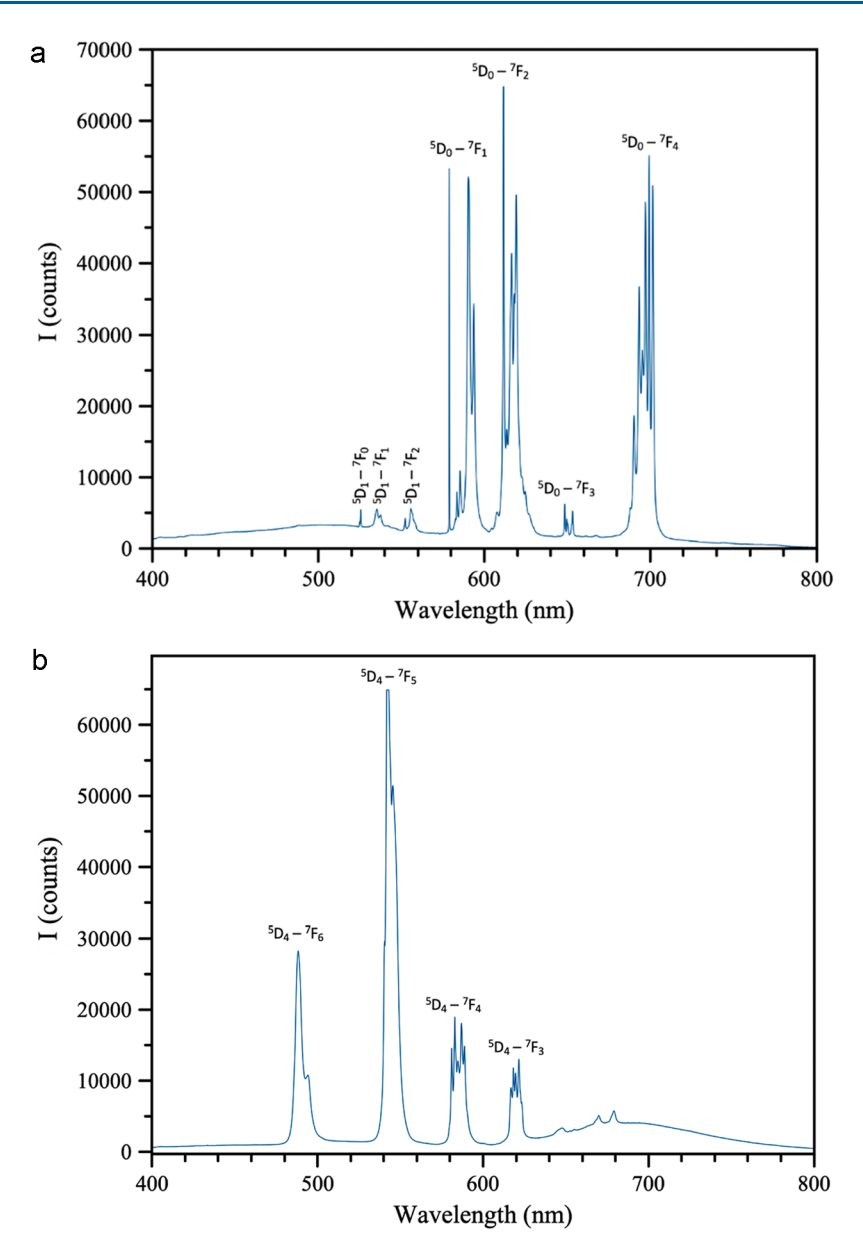


Figure 7. (a) Luminescence spectrum of Cs₂EuCl₅(H₂O)₁₀. (b) Luminescence spectrum of Cs₁₀Tb₂Cl₁₇(H₂O)₁₄(H₃O).

respectively. Generally, in compounds containing Eu environments with inversion symmetry, the intensity of the ${}^5D_0-{}^7F_1$ magnetic dipole transition dominates over the ${}^5D_0-{}^7F_2$ electric dipole transition that is a forbidden transition based on selection rules. However, when the Eu sits on a site with no inversion center, these selection rules are overruled by a forced electric dipole emission and the ${}^5D_0-{}^7F_2$ emission is dominant. In $Cs_2EuCl_5(H_2O)_{10}$, the Eu environment lacks centrosymmetry (Wyckoff site 4c, site symmetry of 2) explaining the high intensity of the ${}^5D_0-{}^7F_2$ transition.

Figure 7b shows the emission spectrum of $Cs_{10}Tb_2Cl_{17}(H_2O)_{14}(H_3O)$ when excited by 365 nm UV light. The emission spectrum is characterized by four major bands, a doublet at 486 and 492 nm, an intense doublet at 541 and 548 nm, and two relatively weak bands centered at 585 and 620 nm, which are attributed to the ${}^5D_4-{}^7F_6$, ${}^5D_4-{}^7F_5$, ${}^5D_4-{}^7F_4$, and ${}^5D_4-{}^7F_3$ transitions, respectively. The broadening of bands, as compared to $Cs_2EuCl_5(H_2O)_{10}$, might be due to the higher multiplicity of the 5D_4 excited state as well as

the efficient migration of self-trapped excitonic energy between the isolated metal centers. $^{48}\,$

The scintillation response of $Cs_{10}Tb_2Cl_{17}(H_2O)_{14}(H_3O)$ in powder form was investigated under X-ray irradiation (RL measurements). Figure 8b illustrates the visual aspect of the scintillation that is dominated by green emission from Tb³⁺ ions, while Figure 9a highlights the three main emission lines. RL measurements were executed at several different times, revealing a monotonic decrease in intensity of the Tb³⁺ emission lines. This behavior is highlighted in Figure 9b and related to the instability of this compound when exposed to ambient conditions. Of the very first RL measurement, the 300−750 nm spectral integral yielded ~16% of that of BGO powder. It was estimated that ~4 min passed between removing the sample from dry ice storage and starting the RL measurement. Because a 6 min exposure to ambient conditions led to a decay of ~4% of the peak intensity at 541 nm of the first measurement, the value of 16% is a reasonable

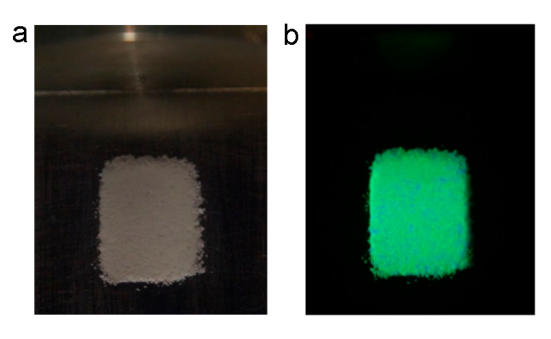


Figure 8. (a) Optical image of the powdered sample of $Cs_{10}Tb_2Cl_{17}(H_2O)_{14}(H_3O)$ in the absence of X-rays. (b) Optical image of the scintillating powdered sample in the presence of X-rays.

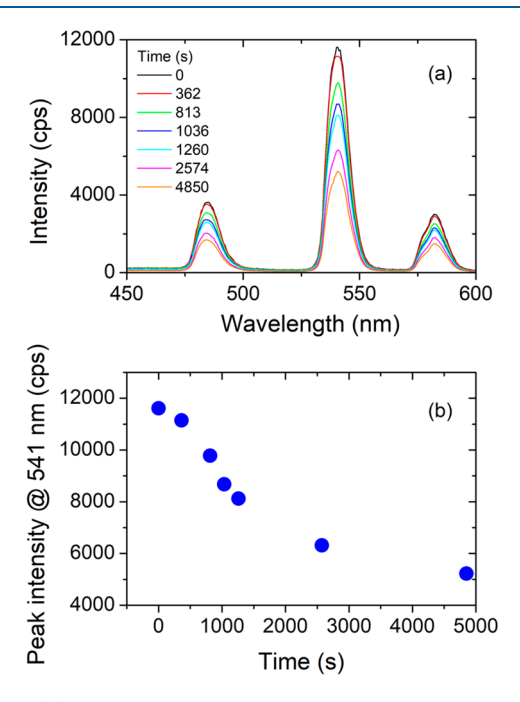


Figure 9. (a) RL spectra highlighting the main luminescence lines of Tb³⁺ ($^5D_4 \rightarrow ^7F_J$, with J=4, 5, and 6 from higher to lower wavelengths) obtained at different times. (b) Peak intensity of the main line at 541 nm ($^5D_4 \rightarrow ^7F_5$) as a function of time.

estimate of the relative luminosity of pristine $Cs_{10}Tb_2Cl_{17}(H_2O)_{14}(H_3O)$ to BGO powder.

CONCLUSIONS

A series of new ternary lanthanide-based chlorides, $Cs_2EuCl_5(H_2O)_{10}$, $Cs_7LnCl_{10}(H_2O)_8$ (Ln = Gd or Ho), $Cs_{10}Tb_2Cl_{17}(H_2O)_{14}(H_3O)$, $Cs_2DyCl_5(H_2O)_6$, $Cs_8Er_3Cl_{17}(H_2O)_{25}$, and $Cs_5Ln_2Cl_{11}(H_2O)_{17}$ (Ln = Y, Lu, or Yb), were synthesized by a facile solution route and structurally characterized. These compounds consist of isolated lanthanide polyhedra that are linked together by Cs-Cl/Cs-O bonds as well as extensive hydrogen bonding to form complex structures. $Cs_2EuCl_5(H_2O)_{10}$ and $Cs_{10}Tb_2Cl_{17}(H_2O)_{14}(H_3O)$ luminesce and exhibit sharp emission peaks in the UV region corresponding to the respective trivalent lanthanide cations. When exposed to laboratory X-rays, crystals of $Cs_{10}Tb_2Cl_{17}(H_2O)_{14}(H_3O)$ scintillate, emitting intense green light, and the integral RL emission was ~16% of BGO powder.

ASSOCIATED CONTENT

Supporting Information

The Supporting Information is available free of charge at https://pubs.acs.org/doi/10.1021/acs.inorgchem.1c02004.

Powder X-ray diffraction patterns, EDS results, and crystallographic tables and information (PDF)

Accession Codes

CCDC 2094750, 2094756, 2094761–2094762, 2094775, 2094777–2094778, 2094788, and 2094798 contain the supplementary crystallographic data for this paper. These data can be obtained free of charge via www.ccdc.cam.ac.uk/data_request/cif, or by emailing data_request@ccdc.cam.ac.uk, or by contacting The Cambridge Crystallographic Data Centre, 12 Union Road, Cambridge CB2 1EZ, UK; fax: +44 1223 336033.

AUTHOR INFORMATION

Corresponding Author

Hans-Conrad zur Loye — Department of Chemistry and Biochemistry, University of South Carolina, Columbia, South Carolina 29208, United States; orcid.org/0000-0001-7351-9098; Email: zurloye@mailbox.sc.edu

Authors

Gyanendra B. Ayer — Department of Chemistry and Biochemistry, University of South Carolina, Columbia, South Carolina 29208, United States

Mark D. Smith – Department of Chemistry and Biochemistry, University of South Carolina, Columbia, South Carolina 29208, United States

Luiz G. Jacobsohn — Department of Materials Science and Engineering, Clemson University, Clemson, South Carolina 29634-0971, United States

Gregory Morrison — Department of Chemistry and Biochemistry, University of South Carolina, Columbia, South Carolina 29208, United States; ⊙ orcid.org/0000-0001-9674-9224

Hunter B. Tisdale – Department of Chemistry and Biochemistry, University of South Carolina, Columbia, South Carolina 29208, United States

Logan S. Breton – Department of Chemistry and Biochemistry, University of South Carolina, Columbia, South Carolina 29208, United States

Weiguo Zhang – Department of Chemistry, University of Houston, Houston, Texas 77004, United States

P. Shiv Halasyamani — Department of Chemistry, University of Houston, Houston, Texas 77004, United States;
orcid.org/0000-0003-1787-1040

Complete contact information is available at: https://pubs.acs.org/10.1021/acs.inorgchem.1c02004

Notes

The authors declare no competing financial interest.

ACKNOWLEDGMENTS

Financial support for this work provided by the National Science Foundation under Grants DMR-1806279, DMR-1653016, and OIA-1655740 is gratefully acknowledged. Syntheses, structure determination, and photoluminescence measurements were performed at the University of South Carolina. Emission spectra of scintillation were measured at Clemson. SHG measurements were performed at the

University of Houston. P.S.H. and W.Z. thank the Welch Foundation (Grant E-1457) and the NSF (DMR-2002319) for support.

REFERENCES

- (1) Nikl, M.; Yoshikawa, A. Recent R&D Trends in Inorganic Single-Crystal Scintillator Materials for Radiation Detection. *Adv. Opt. Mater.* **2015**, 3, 463–481.
- (2) van Eijk, C. W. E. Inorganic Scintillators in Medical Imaging. *Phys. Med. Biol.* **2002**, 47, R85–R106.
- (3) Eriksson, L.; Melcher, C. L.; Eriksson, M.; Rothfuss, H.; Grazioso, R.; Aykac, M. Design Considerations of Phoswich Detectors for High Resolution Positron Emission Tomography. *IEEE Trans. Nucl. Sci.* **2009**, *56*, 182–188.
- (4) Touš, J.; Blažek, K.; Pína, L.; Sopko, B. High-resolution imaging of biological and other objects with an X-ray digital camera. *Appl. Radiat. Isot.* **2010**, *68*, 651–653.
- (5) Cao, F.; Yu, D.; Ma, W.; Xu, X.; Cai, B.; Yang, Y. M.; Liu, S.; He, L.; Ke, Y.; Lan, S.; Choy, K. L.; Zeng, H. Shining Emitter in a Stable Host: Design of Halide Perovskite Scintillators for X-ray Imaging from Commercial Concept. ACS Nano 2020, 14, 5183–5193.
- (6) O'Nions, K.; Pitman, R.; Marsh, C. Science of Nuclear Warheads. *Nature* **2002**, 415, 853–857.
- (7) West, H. I.; Meyerhof, W. E.; Hofstadter, R. Detection of X-rays by means of NaI(Tl) scintillation counters. *Phys. Rev.* **1951**, *81*, 141–142.
- (8) Nagarkar, V. V.; Gupta, T. K.; Miller, S. R.; Klugerman, Y.; Squillante, M. R.; Entine, G. Structured CsI(Tl) scintillators for X-ray imaging applications. *IEEE Trans. Nucl. Sci.* **1998**, *45*, 492–496.
- (9) van Loef, E. V. D.; Dorenbos, P.; van Eijk, C. W. E.; Krämer, K.; Güdel, H. U. High-energy-resolution scintillator: Ce³⁺ activated LaBr₃. *Appl. Phys. Lett.* **2001**, *79*, 1573–75.
- (10) Alekhin, M. S.; de Haas, J. T. M.; Kramer, K. W.; Dorenbos, P. Scintillation Properties of and Self Absorption in SrI₂:Eu²⁺. *IEEE Trans. Nucl. Sci.* **2011**, *58*, 2519–2527.
- (11) Stand, L.; Zhuravleva, M.; Chakoumakos, B.; Johnson, J.; Loyd, M.; Wu, Y.; Koschan, M.; Melcher, C. L. Crystal Growth and Scintillation Properties of Eu²⁺ doped Cs₄CaI₆ and Cs₄SrI₆. *J. Cryst. Growth* **2018**, 486, 162–168.
- (12) Burachas, S. P.; Danevich, F. A.; Georgadze, A. S.; Klapdor-Kleingrothaus, H. V.; Kobychev, V. V.; Kropivyansky, B. N.; Kuts, V. N.; Muller, A.; Muzalevsky, V. V.; Nikolaiko, A. S.; Ponkratenko, O. A.; Ryzhikov, V. D.; Sai, A. S.; Solsky, I. M.; Tretyak, V. I.; Zdesenko, Y. G. Large volume CdWO₄ crystal scintillators. *Nucl. Instrum. Methods Phys. Res., Sect. A* 1996, 369, 164–168.
- (13) Drozdowski, W.; Wojtowicz, A. J.; Kaczmarek, S. Ł. M.; Berkowski, M. Scintillation yield of Bi₄Ge₃O₁₂ (BGO) pixel crystals. *Phys. B* **2010**, 405, 1647–1651.
- (14) Morrison, G.; Latshaw, A. M.; Spagnuolo, N. R.; zur Loye, H.-C. Observation of Intense X-ray Scintillation in a Family of Mixed Anion Silicates, Cs₃RESi₄O₁₀F (RE = Y, Eu-Lu), Obtained via an Enhanced Flux Crystal Growth Technique. *J. Am. Chem. Soc.* **2017**, 139, 14743–14748.
- (15) Ayer, G. B.; Klepov, V. V.; Smith, M. D.; Hu, M.; Yang, Z.; Martin, C. R.; Morrison, G.; zur Loye, H.-C. BaWO₂F₄: a mixed anion X-ray scintillator with excellent photoluminescence quantum efficiency. *Dalton Trans.* **2020**, *49*, 10734-10739.
- (16) Lian, L.; Zheng, M.; Zhang, P.; Zheng, Z.; Du, K.; Lei, W.; Gao, J.; Niu, G.; Zhang, D.; Zhai, T.; Jin, S.; Tang, J.; Zhang, X.; Zhang, J. Photophysics in $Cs_3Cu_2X_5$ (X = Cl, Br, or I): Highly Luminescent Self-Trapped Excitons from Local Structure Symmetrization. *Chem. Mater.* **2020**, 32, 3462–3468.
- (17) Birowosuto, M. D.; Cortecchia, D.; Drozdowski, W.; Brylew, K.; Lachmanski, W.; Bruno, A.; Soci, C. X-ray Scintillation in Lead Halide Perovskite Crystals. Sci. Rep. 2016, 6, 37254.
- (18) Yu, D.; Wang, P.; Cao, F.; Gu, Y.; Liu, J.; Han, Z.; Huang, B.; Zou, Y.; Xu, X.; Zeng, H. Two-dimensional halide perovskite as β -ray

- scintillator for nuclear radiation monitoring. Nat. Commun. 2020, 11, 3395
- (19) Zhou, Y.; Chen, J.; Bakr, O. M.; Mohammed, O. F. Metal Halide Perovskites for X-ray Imaging Scintillators and Detectors. *ACS Energy Lett.* **2021**, *6*, 739–768.
- (20) Zhou, F.; Li, Z.; Lan, W.; Wang, Q.; Ding, L.; Jin, Z. Halide Perovskite, a Potential Scintillator for X-Ray Detection. *Small Methods* **2020**, *4*, 2000506.
- (21) Xie, A.; Maddalena, F.; Witkowski, M. E.; Makowski, M.; Mahler, B.; Drozdowski, W.; Springham, S. V.; Coquet, P.; Dujardin, C.; Birowosuto, M. D.; Dang, C. Library of Two-Dimensional Hybrid Lead Halide Perovskite Scintillator Crystals. *Chem. Mater.* **2020**, 32, 8530–8539.
- (22) Xu, L.-J.; Lin, X.; He, Q.; Worku, M.; Ma, B. Highly efficient eco-friendly X-ray scintillators based on an organic manganese halide. *Nat. Commun.* **2020**, *11*, 4329.
- (23) Li, S.; Xu, J.; Li, Z.; Zeng, Z.; Li, W.; Cui, M.; Qin, C.; Du, Y. One-Dimensional Lead-Free Halide with Near-Unity Greenish-Yellow Light Emission. *Chem. Mater.* **2020**, *32*, 6525–6531.
- (24) He, Q.; Zhou, C.; Xu, L.; Lee, S.; Lin, X.; Neu, J.; Worku, M.; Chaaban, M.; Ma, B. Highly Stable Organic Antimony Halide Crystals for X-ray Scintillation. *ACS Mater. Lett.* **2020**, *2*, 633–638.
- (25) Zheng, W.; Zhou, S.; Chen, Z.; Hu, P.; Liu, Y.; Tu, D.; Zhu, H.; Li, R.; Huang, M.; Chen, X. Sub-10 nm Lanthanide-Doped CaF₂ Nanoprobes for Time-Resolved Luminescent Biodetection. *Angew. Chem.* **2013**, *125*, 6803–6808.
- (26) Wang, L.; Li, Y. Controlled Synthesis and Luminescence of Lanthanide Doped NaYF₄ Nanocrystals. *Chem. Mater.* **2007**, *19*, 727–734
- (27) Mir, W. J.; Sheikh, T.; Arfin, H.; Xia, Z.; Nag, A. Lanthanide doping in metal halide perovskite nanocrystals: spectral shifting, quantum cutting and optoelectronic applications. *NPG Asia Mater.* **2020**, *12*, 9.
- (28) Khan, A.; Rooh, G.; Kim, H. J.; Kim, S. Ce^{3+} -activated Tl_2GdCl_5 : Novel halide scintillator for X-ray and γ -ray detection. *J. Alloys Compd.* **2018**, 741, 878–882.
- (29) Huang, J.; Lei, T.; Siron, M.; Zhang, Y.; Yu, S.; Seeler, F.; Dehestani, A.; Quan, L. N.; Schierle-Arndt, K.; Yang, P. Lead-free Cesium Europium Halide Perovskite Nanocrystals. *Nano Lett.* **2020**, 20, 3734–3739.
- (30) APEX3 version 2019.1-0 and SAINT+ version 8.40A; Bruker Nano, Inc.: Madison, WI, 2019.
- (31) Krause, L.; Herbst-Irmer, R.; Sheldrick, G. M.; Stalke, D. Comparison of Silver and Molybdenum Microfocus X-Ray Sources for Single-Crystal Structure Determination. *J. Appl. Crystallogr.* **2015**, 48 (1), 3–10.
- (32) Sheldrick, G. M. Crystal Structure Refinement with SHELXT. Acta Crystallogr., Sect. A: Found. Adv. 2015, 71 (1), 3-8.
- (33) Sheldrick, G. M. Crystal Structure Refinement with SHELXL. Acta Crystallogr., Sect. C: Struct. Chem. 2015, 71 (1), 3–8.
- (34) Dolomanov, O. V.; Bourhis, L. J.; Gildea, R. J.; Howard, J. A. K.; Puschmann, H. OLEX2: a complete structure solution, refinement and analysis program. *J. Appl. Crystallogr.* **2009**, *42*, 339–341.
- (35) Ayer, G. B.; Klepov, V. V.; Pace, K. A.; zur Loye, H.-C. Quaternary Cerium(IV) Containing Fluorides Exhibiting Ce₃F₁₆ Sheets and Ce₆F₃₀ Frameworks. *Dalton Trans.* **2020**, *49*, 5898–5905.
- (36) Hancock, J. C.; Nisbet, M. L.; Zhang, W.; Halasyamani, P. S.; Poeppelmeier, K. R. Periodic Tendril Perversion and Helices in the $AMoO_2F_3$ (A = K, Rb, NH₄, Tl) Family. *J. Am. Chem. Soc.* **2020**, *142*, 6375–6380.
- (37) Pace, K. A.; Klepov, V. V.; Deason, T. K.; Smith, M. D.; Ayer, G. B.; Diprete, D. P.; Amoroso, J. W.; zur Loye, H.-C. Expansion of the Na₃M^{II}(Ln/An)₆F₃₀ Series: Incorporation of Plutonium into a Highly Robust and Stable Framework. *Chem. Eur. J.* **2020**, *26*, 12941–12944.
- (38) Ayer, G. B.; Klepov, V. V.; Smith, M. D.; zur Loye, H.-C. Mild Hydrothermal Synthesis of the Complex Hafnium-Containing Fluorides $Cs_2[M(H_2O)_6][Hf_2F_{12}]$ (M = Ni, Co, Zn), CuHfF₆(H₂O)₄,

- and Cs₂Hf₃Mn₃F₂₀ Based on HfF₇ and HfF₆ Coordination Polyhedra. *Inorg. Chem.* **2019**, *58*, 13049–13057.
- (39) Hahn, F.; Massa, W. Topotactical Dehydration of Cs₂MnF₅.H₂O to Cs₂MnF₅ and the Crystal Structures of Both Compounds. Z. Naturforsch., B. J. Chem. Sci. **1990**, 45, 1341–1348.
- (40) Reuter, G.; Frenzen, G. The Thermal Dehydration of Cs₃LnCl₆·3H₂O to Cs₃LnCl₆ (Ln = La-Nd) and Their Crystal Structures. *J. Solid State Chem.* **1995**, *116*, 329–334.
- (41) Reuter, G.; Fink, H.; Frenzen, G. The Crystal Structures of the Hydrated Alkalimetal-/Rare Earth(III) Chlorides $ALnCl_4\cdot 4H_2O$ (A= NH₄, K, Rb, Cs; Ln = La–Sm) and CsLaCl₄·3H₂O. *J. Solid State Chem.* **1996**, 126, 44–49.
- (42) Klepov, V. V.; Breton, L. S.; Pace, K. A.; Kocevski, V.; Besmann, T. M.; zur Loye, H.-C. Size-Driven Stability of Lanthanide Thiophosphates Grown from an Iodide Flux. *Inorg. Chem.* **2019**, *58*, 6565–6573.
- (43) Klepov, V. V.; Pace, K. A.; Breton, L. S.; Kocevski, V.; Besmann, T. M.; zur Loye, H.-C. Nearly Identical but Not Isotypic: Influence of Lanthanide Contraction on Cs₂NaLn(PS₄)₂ (Ln = La-Nd, Sm, and Gd-Ho). *Inorg. Chem.* **2020**, *59*, 1905–1916.
- (44) Meyer, G. Cs₂DyCl₅, an ino-chlorodysprosate (III) with an extended cis-two-single-octahedron chain. *Z. Anorg. Allg. Chem.* **1980**, 469, 149–158.
- (45) Latshaw, A. M.; Chance, W. M.; Trenor, N.; Morrison, G.; Smith, M. D.; Yeon, J.; Williams, D. E.; zur Loye, H.-C. $A_5RE_4X[TO_4]_4$ crystal growth and photoluminescence. Hydroflux synthesis of sodium rare earth silicate hydroxides. *CrystEngComm* **2015**, *17*, 4691–4698.
- (46) Shao, B.; Zhao, Q.; Guo, N.; Jia, Y.; lv, W.; Jiao, M.; Lü, W.; You, H. YF₃:Eu³⁺ Micro-Single Crystals: Fine Morphological Tuning and Luminescence Properties. *Cryst. Growth Des.* **2013**, *13*, 3582–3587.
- (47) Blasse, G.; Grabmaier, B. C. Luminescent Materials; Springer: Berlin, 1994.
- (48) Petit, S.; Baril-Robert, F.; Pilet, G.; Reber, C.; Luneau, D. Luminescence spectroscopy of europium(III) and terbium(III) penta-, octa- and nonanuclear clusters with beta-diketonate ligands. *Dalton Trans.* 2009, 6809–6815.